EFFECT OF RESTRAINERS TO MITIGATE POUNDING BETWEEN ADJACENT DECKS SUBJECTED TO A STRONG GROUND MOTION

Kazuhiko KAWASHIMA[1] And Gaku SHOJI[2]

SUMMARY

This paper describes a numerical analysis to clarify the effectiveness of rubber type restrainers to mitigate pounding effect between adjacent decks. Rubber pads are provided at both ends of prestressing cables so that they resist further relative displacement exceeding an initial gap. The stiffness of rubber pad was pre-determined from uniaxial compression loading test of two types of specimens subjected to stress as large as 120MPa. In optimizing the shock absorbing capability, it is required to carefully choose the stress-strain relation of rubber pads. Since various relations are available by properly choosing material and shape of rubber pad, it was assumed in this analysis that the stress-strain relation of the rubber pads be either strain-hardening, strain-softening or elastic type restrainers. A series of nonlinear dynamic analysis was conducted for a bridge system consisting of two five-span continuous bridges with total deck length of 200m supported by elastomeric bearings. Acceleration and relative displacement response of two decks, the impact force, the restrainer force and the curvature ductility factor at the bottoms of piers were analyzed. The multi-degree-of-freedom-lumped-mass model was used to idealize the nonlinear behavior of the bridge. The pounding effect was idealized by the impact spring. The following conclusions were deduced from the analysis; the effect of restrainers is significant in reducing deck response and plastic curvature at pier bottoms; the effect of the energy dissipation in the devices to the total energy dissipation is less significant because poundings occur only twice or three times during an excitation; and the strain-softening device is favorable in reducing the deck response displacement and pounding force.

INTRODUCTION

Since the 1995 Hyogo-ken nanbu earthquake, multi-span continuous bridges supported by the elastomeric bearings have been widely constructed. This is because the lateral force of a superstructure can be distributed to each substructure, and thus it can be avoided to have concentration of the lateral force to several specific substructures. However as the deck length increases, the thermal movement increases. It is therefore required to provide thicker elastomeric bearings to accommodate with the large thermal movement, and this, in turn, results in an increase of the natural period of the bridge. Since the relative displacement of 0.3~0.5m may be induced in a bridge subjected to ground motions recorded in the 1995 Hyogo-ken nanbu earthquake, poundings between adjacent decks or between a deck and an abutment occur. Poundings bring damage at not only expansion joints and contact face of decks but also other elastomeric bearings and columns.

Based on the previous studies [Tseng and Penzien, 1973, Kawashima and Penzien, 1976, Saiidi, et al., 1996, Abdel-Ghaffar, et al., 1997, Desroches and Fenves, 1997], it is obvious that the impact force is very large and

that the shock absorbing mechanism is effective in reducing the pounding effect of structures. Thus it is required to develop an appropriate shock absorbing device that resists to the large impact force with stable hysteretic behavior. Various materials including rubber devices, honeycomb and high-strength reinforced plastic composites have been clarified for the device. It seems that the rubber device is promising because hysteretic

[1] *Department of Civil Engineering, Tokyo Institute of Technology, Tokyo, Japan. Email: kawasima@cv.titech.ac.jp*
[2] *Department of Civil Engineering, Tokyo Institute of Technology, Tokyo, Japan. Email: shoji@cv.titech.ac.jp*

behavior under high compression is stable and that not only strain-hardening hysteresis but strain-softening hysteresis is available.

To develop a rubber shock absorbing device, an uniaxial compression loading test as high as 120MPa was first conducted. Then an effectiveness of the device in reducing bridge response was studied by a nonlinear dynamic response analysis. Effect of the strain-softening hysteresis and the energy dissipation was also studied. This paper presents a series of analysis to clarify the requirements for a rubber shock absorber.

BRIDGE ANALYZED

An urban highway bridge consisting of two 5-span continuous bridges as shown in Fig.1 was analyzed. The superstructure is the same for two bridges, and is of steel plate girder with 5@40m long and 12m wide. Total weight of a 5-span bridge is 31.4MN. The same reinforced concrete columns and foundations as shown in Fig.2 are used in the two bridges. The longitudinal reinforcement ratio ρ_l is 1.31% and the tie reinforcement (volumetric) ratio ρ_s is 0.53% in all columns. Only difference between the two bridges are the stiffness of elastomeric bearings. Five elastomeric bearings with 96mm thick (4 layers@24mm) are installed on each column. However the size of elastomeric bearings is 700mm$\times$700mm in the deck 1 while 990mm$\times$990mm in the deck 2. Thus the stiffness of the elastomeric bearings in deck 2 is about two times that in deck 1.

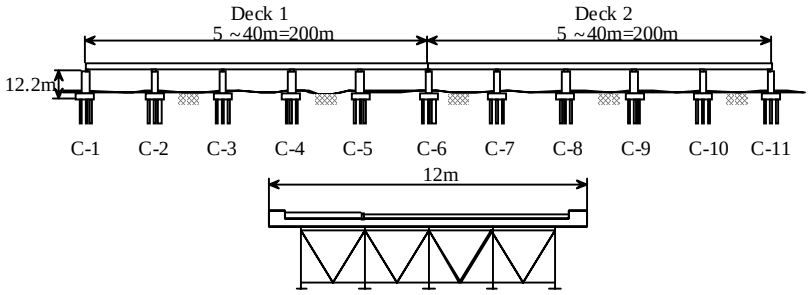

Figure 1: Bridge analyzed

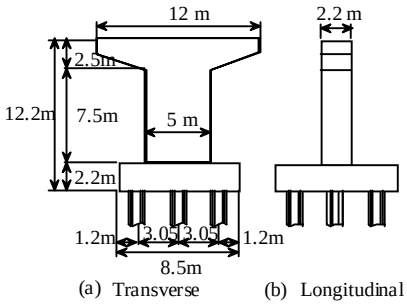

Figure 2: Columns

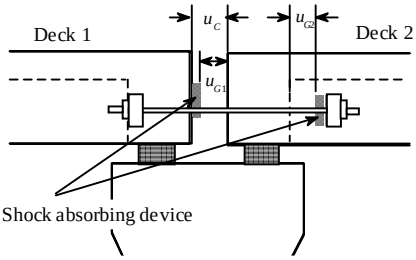

Figure 3: Cable restrainer and cushion

A shock absorbing device (SAD) as shown in Fig. 3 was analyzed in this study. It is of a prestressed cable restrainer and a compression cushion. A natural rubber SAD is set in both the restrainers and the cushion so that it is effective when gap between the decks becomes larger or smaller beyond the movable range of the restrainer and the cushion.

MODELING OF THE BRIDGE

The bridge was idealized by a finite element model as shown in Fig. 4. Response of the bridges in longitudinal direction was analyzed. The stiffness degrading bi-linear model [Takeda, et al., 1970] was assumed in the plastic hinge. The moment-curvature relation in the plastic hinge of columns is computed based on the standard moment-curvature analysis [Japan Road Association, 1996].

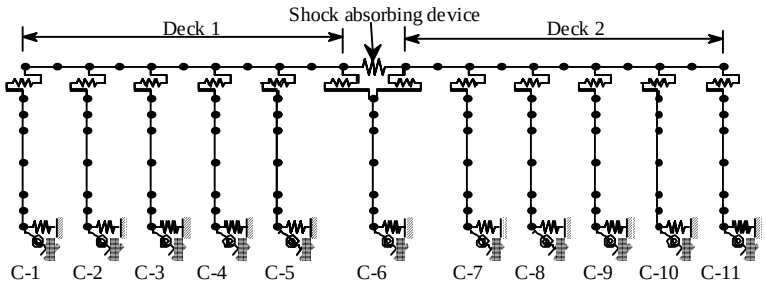

Figure 4: Idealization of the bridge

Pounding between decks was modeled using an impact spring element [Kawashima and Penzien, 1976]. The stiffness of the impact spring element, k_I is given by

$$k_I = \begin{cases} \tilde{k}_I & \Delta u < -u_C \\ 0 & \Delta u \geq -u_C \end{cases} \quad (1)$$

in which $\Delta u = u_2 - u_1$, u_1, u_2 : response displacement of deck 1 and deck 2, respectively, $\tilde{k}_I$: stiffness of an impact spring, and u_C : gap between deck 1 and deck 2.

Ground acceleration spectrally fitted to the design response spectrum for the Type II ground motion at Soil Group I (stiff soil site) [Japan Road Association, 1996] was considered here. Fig. 5 shows the ground motion thus generated and the acceleration response spectrum.

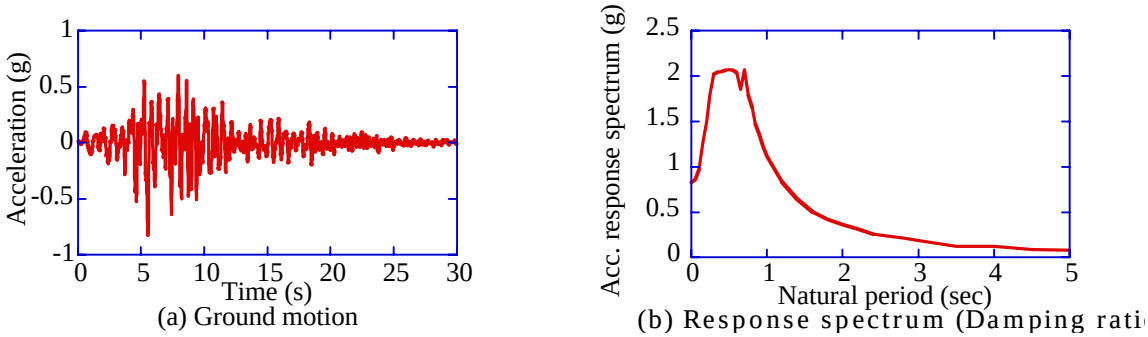

(a) Ground motion (b) Response spectrum (Damping rati

Figure 5: Ground motion and acceleration response spectrum

SHOCK ABSORBING DEVICE

The stiffness of SAD presented in Fig. 3 is given by

$$k_s = \begin{cases} \tilde{k}_s(\Delta\tilde{u}_1) & \Delta u < -u_{G1} \\ 0 & -u_{G1} \leq \Delta u \leq -u_{G2} \\ \tilde{k}_s(\Delta\tilde{u}_2) \cdot k_T / (\tilde{k}_s(\Delta\tilde{u}_2) + k_T) & \Delta u > -u_{G2} \end{cases} \quad (2)$$

in which $\Delta\tilde{u}_1 = |\Delta u - u_{G1}|$, $\Delta\tilde{u}_2 = |\Delta u - u_{G2}|$, $\tilde{k}_s(\Delta\tilde{u}_i)$: stiffness of SAD, k_T : stiffness of a restrainer, and u_{G1}, u_{G2}: clearances of SAD in compression and tension directions, respectively. Because the stiffness $\tilde{k}_s$ of SAD subjected to high compression force depends on the strain, it must be set based on an experiment. Since the stiffness of a restrainer k_T is so large as compared to $\tilde{k}_s(\Delta\tilde{u}_i)$ that assuming $u_G \equiv u_{G1} = u_{G2}$, Eq. (2) becomes

$$k_s = \begin{cases} \tilde{k}_s(\Delta\tilde{u}) & |\Delta\tilde{u}| > u_G \\ 0 & |\Delta\tilde{u}| \leq u_G \end{cases} \quad (3)$$

in which $\Delta\tilde{u} = |\Delta u - u_G|$. Because it is required that the SAD should be effective prior to the direct pounding between the two decks, the clearance of SAD u_G is assumed as $u_G = u_C - h$.

Uniaxial compression loading test was conducted for two SADs with the same geometry and rubber in order to clarify the stiffness of device $\tilde{k}_s(\Delta\tilde{u})$ in Eq. (3). Fig 6(a) shows the stress-strain relation of a SAD under cyclic compression loading. Three-cyclic loading was applied by the rates of 5.0~10.0mm/min. Although the conservative stress in the range of 8~12MPa stress is generally used in design of elastomeric bearings for long-term loading, it is noteworthy that the stress-strain relation of rubber SAD is stable under stress over 120MPa

which resulted in strain over 80%. It may be validated to assume higher stress in design of SAD subjected to short-term seismic loading. It is interesting to note that the energy dissipation occurs even in the natural rubber under high compression strain.

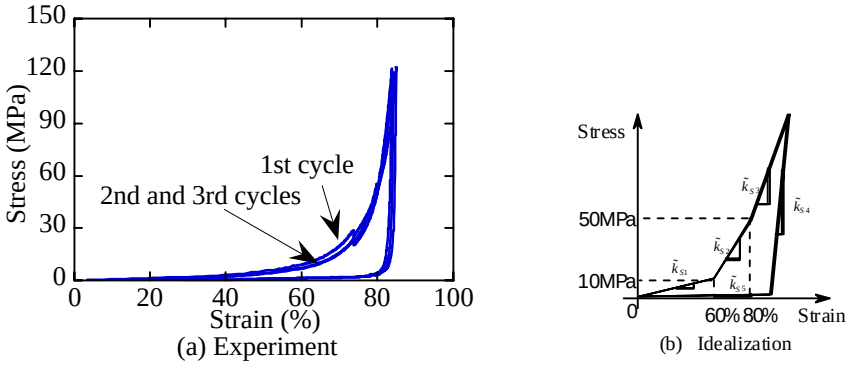

Figure 6: Stress-strain relation of shock absorbing device

From the above compression test, the loading stiffness $\tilde{k}_s^L$ and the unloading stiffness $\tilde{k}_s^{UL}$ of SAD were idealized as (refer to Fig. 6(b))

$$\tilde{k}_s^L = \begin{cases} \tilde{k}_{s1} & 0 \le \varepsilon \le 60\% \\ \tilde{k}_{s2} = 12\tilde{k}_{s1} & 60\% \le \varepsilon \le 80\% \\ \tilde{k}_{s3} = 24\tilde{k}_{s1} & 80\% \le \varepsilon \end{cases} \tag{4}$$

$$\tilde{k}_s^{UL} = \begin{cases} \tilde{k}_{s4} = 48\tilde{k}_{s1} & \sigma \neq 0 \\ \tilde{k}_{s5} = 0 & \sigma = 0 \end{cases} \tag{5}$$

where σ and ε are the stress and strain of SAD, respectively. The $\tilde{k}_{s1}$ for single device with 250mm$\times$150mm section and 100mm thick is 6.25MN/m.

Although Eqs. (4) and (5) provide the strain-hardening (SH) hysteresis, with energy dissipation, it is feasible to develop SAD with arbitrary hysteretic behavior in a certain range. For example, it is possible to develop a strain-softening (SF) SAD by providing many small voids or holes in a SAD. For such purpose, it may be required to use natural rubber with higher modulus. Also it is feasible to develop a SAD with almost elastic (EL) property even under high compression. To analyze what type of hysteretic behavior is appropriate for a SAD, in addition to SH SAD, SF and EL SADs are also clarified in the analysis. To provide the stress-strain relation of the SF and EL SADs the following relations were used assuming that stress at 80% strain is the same among SH, SF and EL SADs (refer to Fig.7) .

SF SAD

$$\tilde{k}_s^L = \begin{cases} \tilde{k}_{s3} = 24\tilde{k}_{s1} & 0 \le \varepsilon \le 20\% \\ \tilde{k}_{s2} = 12\tilde{k}_{s1} & 20\% \le \varepsilon \le \varepsilon_0 \\ \tilde{k}_{s1} & \varepsilon_0 < \varepsilon \end{cases} \tag{6}$$

EL SAD

$$\tilde{k}_s^L = \frac{\sigma_{\max}}{\varepsilon_{\max}} \tag{7}$$

in which $\varepsilon_0 = (\sigma_{\max} - \varepsilon_{\max}\tilde{k}_{s1} + 0.2\tilde{k}_{s2} - 0.2\tilde{k}_{s3})/(\tilde{k}_{s2} - \tilde{k}_{s1})$, and ε_0 : strain where the second stiffness $\tilde{k}_{s2}$ changes to the third stiffness $\tilde{k}_{s3}$.

Furthermore, a SH SAD without energy dissipation was considered in the following analysis to clarify the effect of energy dissipation in the device. For such purpose, it was assumed that the stress-strain relation is provided by Eq. (4) by eliminating Eq. (5).

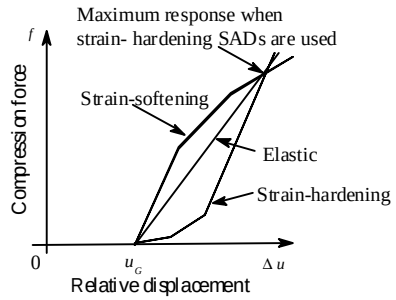

Figure 7: Skeleton curves of strain-hardening, strain-softening, and elastic-type SAD

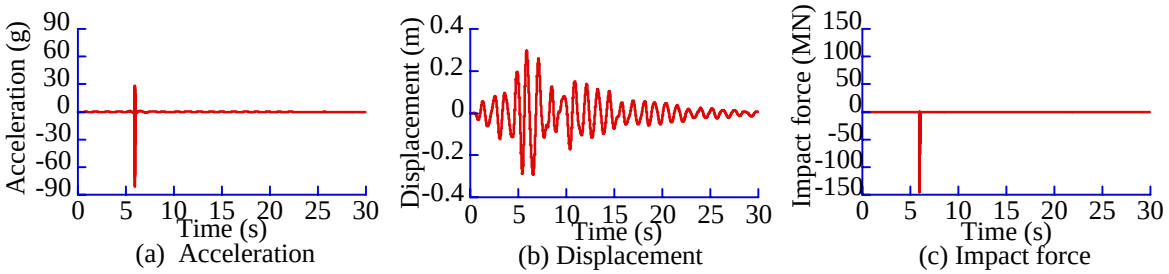

Figure 8: Response of deck 1 without device

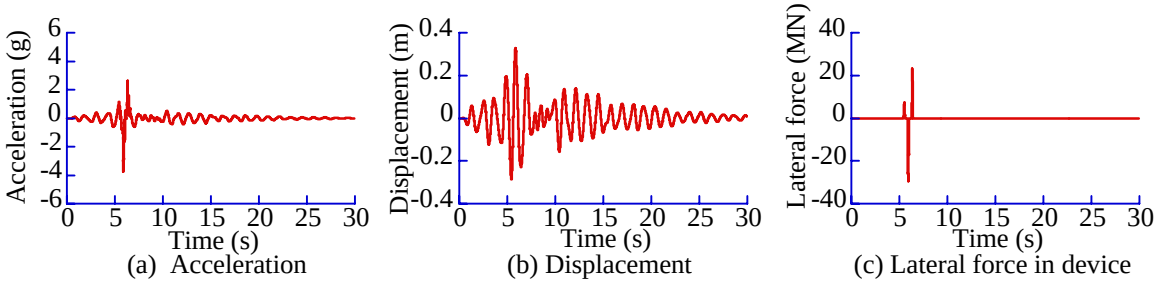

Figure 9: Response of deck 1 with SH SADs

COMPARISONS OF SEISMIC RESPONSE WITH AND WITHOUT DEVICE

Figs. 8 and 9 compare the seismic responses of the bridge with and without SH SAD. It was assumed that 20 250mm x150mm and 100mm thick SADs are provided between the decks, and that u_C is 0.25m and u_G is 0.15m. From Fig. 8, it is seen that a pounding occurred resulting in a large contact force of 146.3MN, 4.7 times deck weight. This developed a spike acceleration with 80.8g at the contact ends of deck. On the other hand, in the bridge with SAD, the peak contact force decreases to 29.6MN resulting in the decrease of deck acceleration to 3.8g. Thus it is apparent that the SADs are effective to reduce the pounding force and the deck acceleration.

Fig. 10 shows the effectiveness of SADs in terms of the plastic flexural curvature at the plastic hinge of columns. Larger inelastic response occurred in column 8 than column 4 because the deck 2 has shorter fundamental natural period than deck 1. It is thus obvious that the plastic flexural deformation in column 8 decreases 22% (from 4.93 to 3.88) by providing the SADs. The curvature ductility slightly decreases in column 4 because the response of column 4 which exhibits smaller response than column 8 slightly increases by providing SADs.

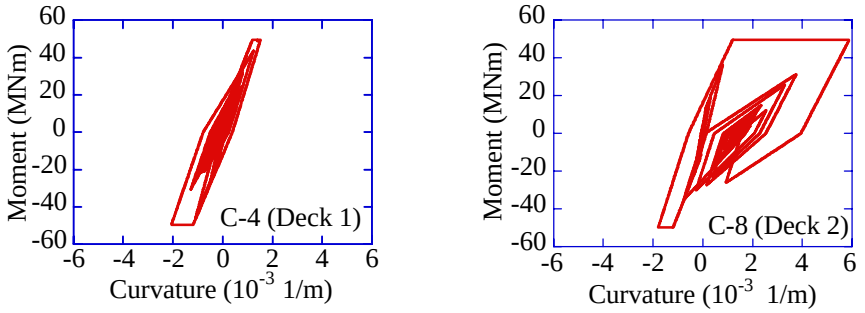

(a) Without device

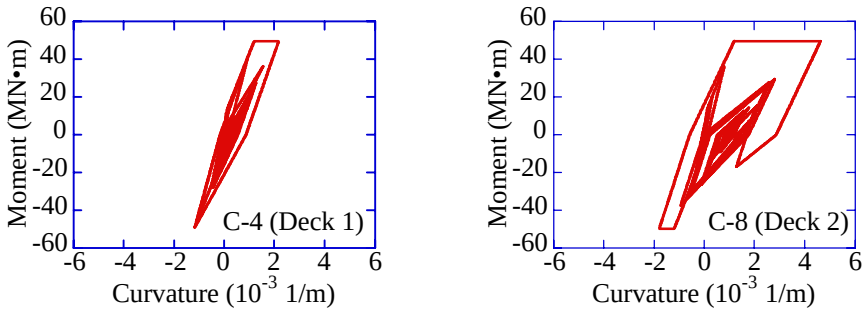

(b) With device

Figure 10: Moment – curvature relation in plastic hinge of column

EFFECT OF ENERGY DISSIPATION IN DEVICE

Fig. 11 shows the effect of energy dissipation of SH SADs in terms of the peak compression force induced in the devices. Being $u_C = 0.25$m and $u_G = 0.15$m, the number of devices was varied as a parameter. It is obvious that the effect of energy dissipation of SADs is less significant in decreasing the compression force in devices.

Total energy dissipated in a bridge system subjected to a ground motion W is given by

$$W = W_D + W_E + W_P + W_S \tag{8}$$

in which W_D: energy dissipation associated with viscous damping, W_E: elastic strain energy in the elastic structural component, W_P: hysteretic energy dissipation in the plastic hinge of columns, and W_S: hysteretic energy dissipation in SADs. W_D, W_E, W_P, and W_S are evaluated by

$$W_D = \int \underline{F}_{Dt}^T \cdot d\underline{u}_{Dt}\,; W_E = \int \underline{F}_{Et}^T \cdot d\underline{u}_{Et}; W_P = \int \underline{F}_{Pt}^T \cdot d\underline{u}_{Pt}\,; W_S = \int \underline{F}_{S}^T \cdot d\underline{u}_{St} \tag{9}$$

in which $\underline{F}_{Dt}^T$, $\underline{F}_{Et}^T$, $\underline{F}_{Pt}^T$, and $\underline{F}_{St}^T$ are the damping force, the restoring force in the elastic components, the restoring force in the plastic hinge of columns, and the lateral force induced in SADs at time t, and $\underline{u}_{Dt}$, $\underline{u}_{Et}$, $\underline{u}_{Pt}$, and $\underline{u}_{St}$ are the displacements corresponding to above forces. One can compute W_D, W_E, W_P, and W_S from Eq. (9) for the bridge with 20 SADs as 15.7MNm, 0.001MNm, 3.04MNm and 0.98MNm, respectively. The energy W_S dissipated in SADs is only 5% of total energy dissipated in the bridge system W. This is the reason why the effect of energy dissipation in SADs is less significant in reducing the impact force. Therefore it may be regarded that the energy dissipation capacity is not the requirement with significant importance for SAD although it contributes in good direction if any.

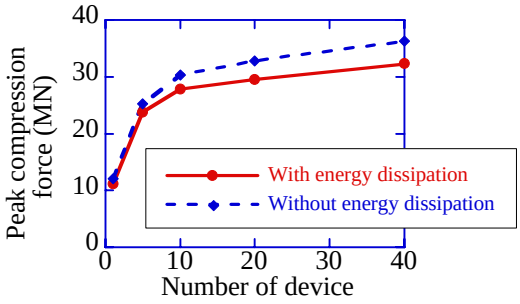

Figure 11: Effect of energy dissipation in SAD on peak compression force

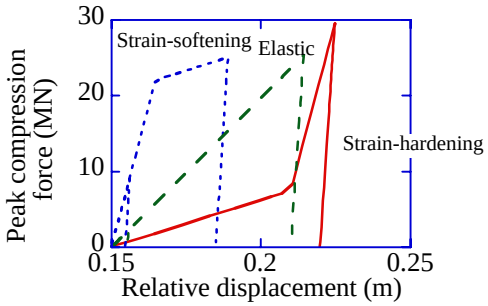

Figure 12: Effect of hysteresis of the device on peak compression force

STRAIN-HARDENING AND STRAIN-SOFTENING DEVICES

Fig. 12 compares the largest hystereses of SH, SF and EL SADs in terms of the peak compression force in the devices. It was assumed in this analysis that 20 SADs are provided with $u_C = 0.25$m and $u_G = 0.15$m. The peak compression force is 29.6MN in SH SAD while it decreases to 25.1MN in SF SAD. The compression force in EL SAD exhibits the middle between the SH SAD and SF SAD. It is seen in Fig.12 that SF SADs are more effective than the SH SADs because SF SADs reduces the relative displacement between the two decks with smaller compression force; the relative displacement is 0.189m when SF SADs are used while it is 0.214m and 0.225m when EL and SH SADs are used, respectively. This is because the restoring force at small relative displacement is higher in SF SADs than other two types SADs.

Fig. 13 shows the moment vs. curvature hysteresis of EL and SF SADs in the plastic hinge of the columns 4 and 8. From Fig.10(b) and Fig.13 the curvature ductility factor is 3.88 in the column 8 when SH SADs are used while it decreases to 2.51 in the same column when SF SADs are used. It is obvious that SF SADs are superior in general than the SH and EL SADs.

CONCLUSIONS

To analyze the effectiveness of a rubber shock absorbing device and to clarify the appropriate hysteretic behavior as well as the energy dissipation capability, a series of nonlinear dynamic response analysis was conducted for a bridge system consisting of two 5-span continuous plate girder bridges. Based on the analysis presented herein, the following conclusions may be deduced :

1. Installation of the shock absorbing device significantly reduces the impact force between the decks. The inelastic response of the columns also decreases by providing the shock absorbing device.
2. The effect of hysteretic energy dissipation in the shock absorbing device on the deck displacement and the inelastic response in the column is less significant. This is because the energy dissipated in the device is only 5% of the total energy dissipation in the bridge.
3. The strain-softening device with the stress-strain relation as shown in Fig.13 may be preferable than the strain-hardening device since it effectively reduces the relative displacement between the two decks with smaller compression force. It is also effective in reducing the plastic flexural curvature in the columns as well as the deck displacement.

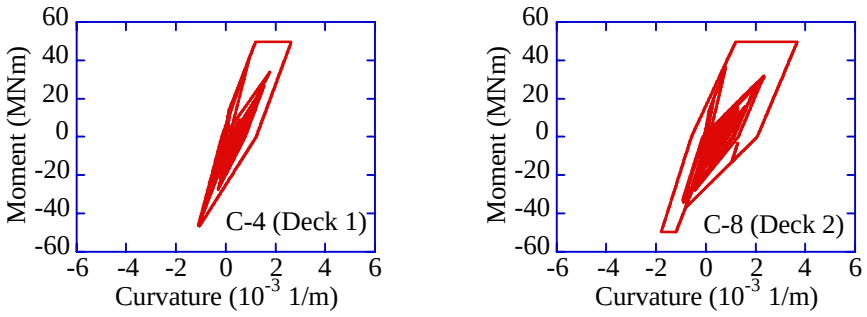

(a) Elastic

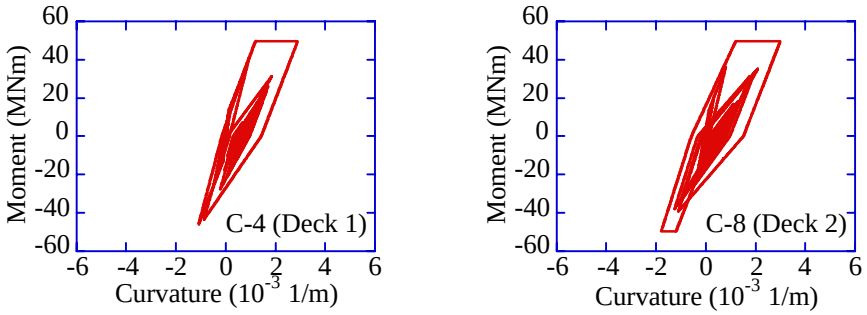

(b) Strain-softening

Figure 13: Effect of hysteresis of SAD on moment – curvature relation at the plastic hinge of columns

REFERENCES

Abdel-Ghaffar, S.M., Maragakis, E. and Saiidi, M. (1997), "Effects of the hinge restrainers on the response of the Aptos Creek bridge during the 1989 Loma Prieta earthquake," *Earthquake Spectra*, 13(2), pp167-189.

Desroches, R. and Fenves, G. L. (1997), "Evaluation of recorded earthquake response of a curved highway bridge," *Earthquake Spectra*, 13(3), pp363-386.

Japan Road Association (1996), "Design Specifications of Highway Bridges."

Kawashima, K. and Penzien, J. (1976), "Correlative investigation on theoretical and experimental dynamic behavior of a model bridge structure," Report No. EERC 76-26, *Earthquake Engineering Research Center, University of California, Berkeley*.

Saiidi, M. S. , Maragakis, E. and Feng, S. (1996), "Parameters in bridge restrainer design for seismic retrofit," *Journal of Structural Engineering*, ASCE, 122(1), pp55-61.

Takeda, T., Sozen, M. A. and Nielsen, N.N. (1970), "Reinforced concrete response to simulated earthquakes," *Proc. of the 3rd Japan Earthquake Symposium*, pp357-364.

Tseng, W. S. and Penzien, J. (1973), "Analytical investigations of the seismic response of long multiple-span highway bridges," Report No. EERC 73-12, *Earthquake Engineering Research Center, University of California, Berkeley.*